

Role of the Tetradecapeptide Repeat Domain of Human Histone Deacetylase 6 in Cytoplasmic Retention*

Received for publication, July 28, 2004, and in revised form, September 1, 2004
Published, JBC Papers in Press, September 3, 2004, DOI 10.1074/jbc.M408583200

Nicholas R. Bertos[‡], Benoit Gilquin[§], Gordon K. T. Chan[¶], Tim J. Yen[¶], Saadi Khochbin[§],
and Xiang-Jiao Yang[‡]||

From the [‡]Molecular Oncology Group, Department of Medicine, McGill University Health Centre, Montreal, Quebec H3A 1A1, Canada, [§]Equipe Chromatine et Expression des Genes, INSERM U309, Institut Albert Bonniot, Faculté de Médecine, Domaine de la Merci, 38706 La Tronche Cedex, France, and [¶]Fox Chase Cancer Center, Philadelphia, Pennsylvania 19111

Histone deacetylase 6 (HDAC6) contains tandem catalytic domains and a ubiquitin-binding zinc finger and displays deacetylase activity toward acetylated microtubules. Here we show that unlike its orthologs from *Caenorhabditis elegans*, *Drosophila*, and mouse, human HDAC6 possesses a tetradecapeptide repeat domain located between the second deacetylase domain and the C-terminal ubiquitin-binding motif. Related to this structural difference, the cytoplasmic localization of human, but not murine, HDAC6 is resistant to treatment with leptomycin B (LMB). Although it is dispensable for the deacetylase and ubiquitin binding activities of human HDAC6, the tetradecapeptide repeat domain displays acetyl-microtubule targeting ability. Moreover, it forms a unique structure and is required for the LMB-resistant cytoplasmic localization of human HDAC6. Besides the tetradecapeptide repeat domain, human HDAC6 possesses two LMB-sensitive nuclear export signals and a nuclear localization signal. These results thus indicate that the cytoplasmic localization for murine and human HDAC6 proteins is differentially regulated and suggest that the tetradecapeptide repeat domain serves as an important sequence element to stably retain human HDAC6 in the cytoplasm.

Lysine acetylation has been shown to regulate functions of histones, about 40 transcription factors, and over 30 other proteins (1). This modification process is reversible and maintained by opposing actions of lysine acetyltransferases and deacetylases *in vivo*. Among the latter are histone deacetylases (HDACs).¹ According to sequence homology to yeast proto-

types, known mammalian HDACs have been grouped into three classes (2–5). Within class II, there are HDAC4, HDAC5, HDAC6, HDAC7, HDAC9, and HDAC10. The catalytic domains of these deacetylases display significant sequence similarity to that of yeast Hda1 (6). Among class II members, HDAC4, HDAC5, HDAC7, and HDAC9 constitute a subclass (IIa), whereas HDAC6 and HDAC10 form class IIb. It is well established now that class IIa members are enzymatic transcriptional corepressors whose functions are regulated by nucleocytoplasmic trafficking (5, 7).

HDAC6, a class IIb member, possesses tandem catalytic domains and a Cys/His-rich motif (8, 9). The Cys/His-rich motif shows significant sequence homology to the BRCA1-associated protein BRAP2 and several ubiquitin-specific proteases, and is known as a DAUP (deacetylase-ubiquitin-specific protease) domain (10), HUB (HDAC6-, USP3- and BRAP2-related) finger (11), ZnF-UBP (ubiquitin C-terminal hydrolase-like zinc finger) (12), PAZ (polyubiquitin-associated zinc finger) (13), and BUZ (bound to ubiquitin zinc finger) (14). It specifically interacts with ubiquitin (12, 13) and may function as a monoubiquitin ligase (15). Related to this, HDAC6 binds to phospholipase A₂-activating protein and p97, both of which have been implicated in regulating ubiquitin-dependent degradation (12). In addition, HDAC6 colocalizes with microtubules and deacetylates α -tubulin to regulate cell motility (16–21), aggresome formation (14), and immune synapse organization (22). Therefore, HDAC6 plays important roles in the cytoplasm.

Inhibition of CRM1-dependent nuclear export results in accumulation of murine HDAC6 (mHDAC6) in the nucleus (23), so its cytoplasmic localization may be regulated. Different from the *Caenorhabditis elegans*, *Drosophila*, and murine orthologs, human HDAC6 (hHDAC6) possesses eight consecutive Ser-Glu-containing tetradecapeptide (SE14) repeats between the second deacetylase domain and the C-terminal ubiquitin-binding zinc finger (11). Here we report that the cytoplasmic localization of hHDAC6 is resistant to treatment with leptomycin B (LMB), demonstrate that the SE14 repeat domain is responsible for this resistance, and show that hHDAC6 possesses intrinsic nuclear import and export signals. Thus, these results unexpectedly reveal that, compared with its murine ortholog, hHDAC6 possesses additional mechanisms for its cytoplasmic retention.

EXPERIMENTAL PROCEDURES

Plasmid Constructs—Mammalian expression plasmids for hHDAC6 and deletion mutants were constructed on pcDNA3.1(-) (Invitrogen) by

* This work was supported by funds from the Canadian Cancer Society through the National Cancer Institute of Canada and from the Canada Foundation for Innovation (to X. J. Y.), a fellowship from Ligue Nationale Contre Cancer-comité de l'Isère and ARC (to B. G.) and a grant from Région Rhône-Alpes-thème prioritaire Cancer (to S. D.). The costs of publication of this article were defrayed in part by the payment of page charges. This article must therefore be hereby marked "advertisement" in accordance with 18 U.S.C. Section 1734 solely to indicate this fact.

|| To whom correspondence should be addressed: Molecular Oncology Group, Royal Victoria Hospital, Rm. H5.41, McGill University Health Centre, 687 Pine Ave. West, Montreal, Quebec H3A 1A1, Canada. Tel.: 514-934-1934 (ext. 34490); Fax: 514-843-1478; E-mail: xiang-jiao.yang@mcgill.ca.

¹ The abbreviations used are: HDAC, histone deacetylase; hHDAC6, human HDAC6; mHDAC6, murine HDAC6; dHDAC6, *Drosophila* HDAC6; SE14, serine-glutamate containing tetradecapeptide; LMB, leptomycin B; HUB, HDAC6-, USP3- and BRAP2-related zinc finger; CRM1, chromosome regulation and maintenance 1; NES, nuclear export signal; NLS, nuclear localization signal; CRS, cytoplasmic reten-

tion signal; ActD, actinomycin D; GFP, green fluorescent protein; PMSF, phenylmethylsulfonyl fluoride; RT, reverse transcription; PBS, phosphate-buffered saline; TSA, trichostatin A.

standard methods. GFP constructs were derived from pEGFP-C2 (BD Biosciences). Additional HDAC6 mutants were generated by PCR with Expand (Roche Applied Science) thermostable DNA polymerase or by site-directed mutagenesis with single-stranded uracil-containing templates and T7 DNA polymerase. Mutations were confirmed by sequencing with T7 Sequenase 2.0 (Amersham Biosciences).

RT-PCR—Total RNA was isolated from murine kidney, liver, and lung using TRIzol reagent (Invitrogen) according to the manufacturer's instructions. RNA quality was assessed by agarose gel electrophoresis and ethidium bromide staining. A One-step RT-PCR kit (Qiagen) was used to amplify cDNA fragments corresponding to nucleotides 2607–3133 of mHDAC6 (GenBank™ accession number NM_010413) with primers NDA57 (5'-TCC TGT ATC AGC TAA GGA AA-3') and NDA58 (5'-GGG TAT TAA AGT CCC CAA AT-3'). An aliquot of 200 ng of RNA was used in a total volume of 10 μ l per RT-PCR. After 30 cycles of amplification in the GeneAmp PCR System 9700 (PerkinElmer Life Sciences), amplified products were analyzed by agarose gel electrophoresis and cloned for subsequent sequencing.

Preparation of Extracts from HeLa S3 Suspension Culture—For suspension culture, adherent cells were harvested by trypsinization and resuspended in Joklik's-modified essential medium (Invitrogen) supplemented with minimum Eagle's medium nonessential amino acids (Invitrogen), 2 mM L-glutamine, 24 mM NaHCO₃, and 5% fetal bovine serum. The suspension culture was grown in spinner flasks at 37 °C with stirring (100 rpm). For extract preparation, cells were harvested at 0.8–1.7 \times 10⁶ cells/ml. Cytoplasmic and nuclear extracts were prepared as described (24).

Sizing Chromatography—Cell extracts were fractionated on a prepacked Superose 6 column (HR 10/30; Amersham Biosciences) linked to a BioLogic protein purification system (Bio-Rad). The column was equilibrated with buffer B (20 mM Tris-HCl, pH 8.0, 10% glycerol, 5 mM MgCl₂, 0.1% Tween 20, 5 mM β -mercaptoethanol, and 0.5 mM PMSF) containing 0.15 M KCl. For extract injection, 0.5- or 1.0-ml static loops were used. For molecular weight calibration of the column, a gel filtration HMW calibration kit (Amersham Biosciences) was used. Fractions were analyzed by SDS-PAGE and Coomassie staining.

Expression of hHDAC6 in Sf9 Cells—The hHDAC6 coding sequence was cloned into pFastBac1 (Invitrogen) along with a C-terminal FLAG tag. Recombinant baculovirus was generated using the Bac-to-Bac Baculovirus Expression System (Invitrogen) and then used to infect Sf9 insect cells, growing as a suspension culture in Grace's insect medium supplemented with 10% fetal bovine serum, 1% Pluronic F68, and antibiotics. 48 h post-infection, cells were harvested and washed once with phosphate-buffered saline (PBS). Extracts were prepared in buffer B containing 0.15 M KCl and subjected to affinity purification on anti-FLAG M2-agarose. Protein purity was assessed by SDS-PAGE and Coomassie staining.

HDAC Assays—HDAC activities were determined by measuring the release of [³H]acetate from [³H]acetyl-histones as described previously (25). Assays were carried out in 0.2 ml of buffer H (50 mM Tris-HCl, pH 7.5, 100 mM NaCl, 0.1 mM EDTA, and 0.1 mM PMSF) containing [³H]acetyl-histones (20,000 dpm). The reaction was allowed to proceed at 37 °C for 2 h and was stopped by the addition of 50 μ l of 0.1 M HCl, 0.16 M acetic acid. Released [³H]acetate was extracted with 0.6 ml of ethyl acetate. After centrifugation, 0.45 ml of the upper organic phase was subjected to liquid scintillation counting.

Tubulin Deacetylation—*In vivo* tubulin deacetylation assays were performed as described (18). For *in vitro* assays, 6-well plates containing COS cells at 75% confluency were transfected with 2 μ g of expression vectors encoding hHDAC6 and mutants. 24 h after transfection, cells were lysed in 50 μ l of lysis buffer (15 mM NaCl, 60 mM KCl, 12% sucrose, 2 mM EDTA, 0.5 mM EGTA, 0.65 mM spermidine, 1 mM dithiothreitol, 0.5 mM PMSF, and 50 ng/ml trichostatin A (TSA)) and kept at room temperature for 30 min prior to the addition of the SDS sample buffer for subsequent SDS-PAGE and Western blotting analysis.

Ubiquitin Binding Assays—Extract preparation and ubiquitin pull-down assays were performed as described previously (12).

Anti-hHDAC6 Antibody Production—The C-terminal 409 residues of hHDAC6 were expressed as a maltose-binding protein fusion and purified as described (26). The purified maltose-binding protein fusion protein was dialyzed against PBS and then injected into a rabbit for antiserum production.

Small Scale Cytoplasmic and Nuclear Fractionation—A procedure described previously (26, 27) was used with minor modifications. Briefly, cultured cells were washed twice with PBS and lysed *in situ* using 0.5 ml of ice-cold hypotonic lysis buffer (20 mM HEPES, pH 7.6, 20% glycerol, 10 mM NaCl, 1.5 mM MgCl₂, 0.2 mM EDTA, 0.1% Triton

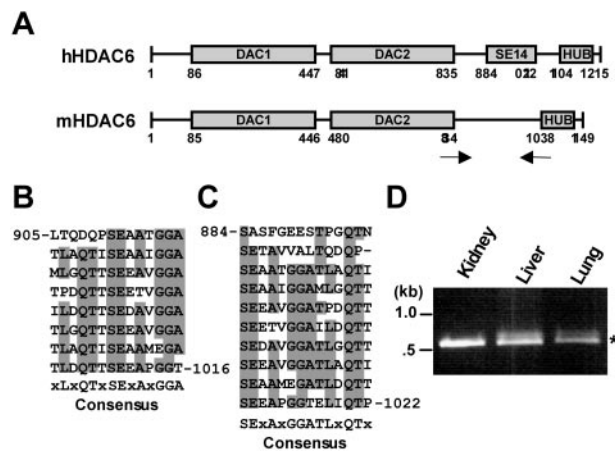


FIG. 1. The SE14 repeat domain is unique to hHDAC6. A, schematic representation of human and mouse HDAC6. DAC1 and DAC2, tandem deacetylase domains; SE14, SE14 repeat domain; and HUB, HDAC6-, USP3-, and BRAP2-related zinc finger. Arrows represent positions of primers used for RT-PCR amplification of a mHDAC6 cDNA fragment. B and C, two potential sequence alignments of the SE14 repeats of hHDAC6. Consensus sequences are also shown. To derive the consensus sequences, a residue was considered to be conserved if it remains unchanged in six (B) or seven (C) repeats. D, RT-PCR was performed with total RNA from indicated murine tissues using primers depicted above. The asterisk marks the predicted size of the RT-PCR fragment based on published mHDAC6 sequences.

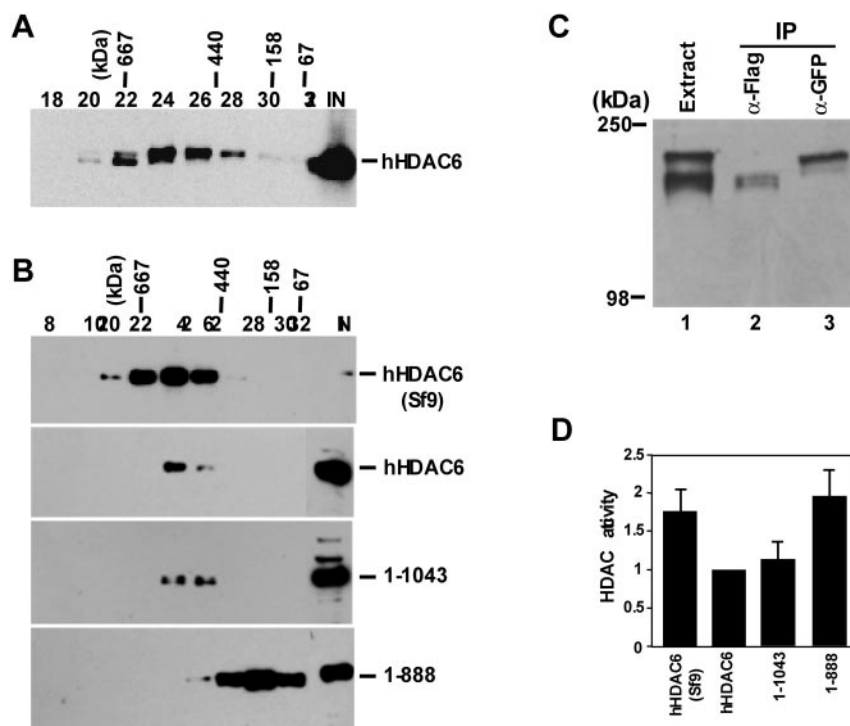
X-100, 25 mM NaF, 25 mM β -glycerophosphate, 1 mM dithiothreitol, and protease inhibitors). After 5 min on ice with occasional agitation, the cell lysate was harvested by scraping and centrifuged for 10 min in a benchtop centrifuge (1,300 \times g) at 4 °C. The supernatant was collected, cleared by high speed centrifugation (10 min at 16,000 \times g) at 4 °C, and saved as the cytoplasmic fraction. The pellet from the low speed centrifugation was suspended in 0.5 ml of hypotonic lysis buffer containing 0.5 M NaCl and rotated for 30 min at 4 °C. After the high speed centrifugation, supernatants were collected as nuclear extracts.

Fluorescence Microscopy—Green fluorescence and indirect immunofluorescence microscopic analyses were performed as described (28).

RESULTS

SE14 Repeat Domain of hHDAC6—Besides its tandem catalytic domains and the ubiquitin-binding zinc finger, hHDAC6 possesses eight SE14 repeats with the consensus sequence XLXQTXSEXAXGGA, where X represents any amino acid residue and invariant residues are shown in boldface (Fig. 1, A and B). A slightly different alignment allows 10 repeats with the consensus sequence SEXAXGGATLXQTX (Fig. 1C). It is presently unclear which alignment represents the structure of this domain, but the presence of such repeats suggests that this domain may have a unique structure and thereby play a role in regulating the function of hHDAC6. Most intriguingly, this SE14 repeat domain is not present in the published sequences of *C. elegans*, *Drosophila*, mouse, and rat HDAC6 proteins (GenBank™ accession numbers NP_500788, NP_034543 and XP_228733 (8, 29). To confirm that the published mouse HDAC6 sequence (8) does not just represent an isoform lacking an SE14 repeat domain, total RNA was isolated from three murine tissues and subjected to RT-PCR with primers flanking the potential SE14 repeat domain (Fig. 1A). Based on the published mouse HDAC6 sequence (8), the fragment was predicted to be 530 bp. If there were an isoform with an SE14 repeat domain, the corresponding cDNA fragment would be ~1 kb. As shown in Fig. 1D, only a fragment of ~530 bp was amplified from all three tissues. DNA sequencing confirmed that this fragment corresponds to the published mouse HDAC6 sequence. Exon-intron organization of the *hHDAC6* gene and RT-PCR analysis indicated that there are no alternatively spliced hHDAC6 isoforms lacking the SE14 repeat domain

FIG. 2. The SE14 repeat domain affects the apparent size, but not the deacetylase activity, of hHDAC6. *A*, HeLa S3 cytoplasmic extracts were fractionated on a Superose 6 column, and resulting fractions as well as extracts were analyzed by Western blotting with anti-hHDAC6 antibody. Peak migration positions of native molecular weight standards are depicted at *top*. *B*, extracts from Sf9 insect cells (*top*) expressing FLAG-tagged hHDAC6 and from 293 cells (*lower three panels*) expressing FLAG-tagged hHDAC6 and two deletion mutants were fractionated as in *A*. The resulting fractions were analyzed by Western blotting with anti-FLAG M2 antibody. *C*, extracts from 293 cells expressing GFP-hHDAC6 and FLAG-hHDAC6 were subject to immunoprecipitation (IP) with anti-FLAG (lane 2) or anti-GFP antibody (lane 3), followed by immunoblotting with anti-hHDAC6 antibody. *D*, FLAG-tagged hHDAC6 and its deletion mutants were expressed in Sf9 and 293 cells and affinity-purified on M2 agarose prior to HDAC assays. Relative protein concentrations were assessed by immunoblotting with anti-FLAG antibody and used for normalization. The activity of hHDAC6 expressed in and affinity-purified from 293 cells was arbitrarily set to 1.0.



(data not shown). Therefore, the SE14 repeat domain is present in human, but not murine, HDAC6.

Role of the SE14 Repeat Domain in Modulating the Apparent Size of HDAC6—The unusual feature of the SE14 repeat domain suggests that it may affect the overall structure of full-length hHDAC6. To address this, size-exclusion chromatography was performed to determine the apparent size of hHDAC6. HeLa S3 cell extracts were fractionated on a Superose 6 column, and the resulting fractions were analyzed by immunoblotting with anti-hHDAC6 antibody. Endogenous hHDAC6 was detected in fractions 24–26, corresponding to a molecular mass of ~500 kDa (Fig. 2*A*). This is larger than the predicted molecular mass of monomeric hHDAC6 (~150 kDa). To assess whether the apparent size of native hHDAC6 is due to association with other proteins, we expressed FLAG-tagged hHDAC6 in Sf9 insect cells. Extracts from these cells were fractionated on the same Superose 6 column, and the resulting fractions were analyzed by immunoblotting with anti-FLAG antibody. Similar to what was observed with endogenous hHDAC6, FLAG-tagged hHDAC6 from Sf9 cells peaked at fraction 24, corresponding to a molecular mass of ~500 kDa (Fig. 2*B*, *top*). No signal was detected at the expected molecular mass of monomeric hHDAC6 (~150 kDa). Coomassie staining of FLAG-tagged hHDAC6, affinity-purified from Sf9 cells, revealed that the purified protein is almost homogeneous (data not shown), suggesting that the apparent size of hHDAC6 is not due to association with other proteins.

To investigate whether the apparent size of hHDAC6 is due to oligomerization, we determined its self-association ability. For this, FLAG-tagged hHDAC6 was coexpressed with GFP-hHDAC6 in 293 cells. These two fusion proteins were immunoprecipitated with anti-FLAG and anti-GFP antibodies, and immunoblotting was performed using anti-hHDAC6 antibody. As shown in Fig. 2*C*, FLAG-hHDAC6 and GFP-hHDAC6 did not coimmunoprecipitate with each other, indicating that they do not oligomerize. In agreement with this, *Drosophila* HDAC6 is mainly monomeric (29).

To assess how the SE14 repeat domain contributes to the apparent size of hHDAC6, two C-terminal deletion mutants,

1–1043 and 1–888, were utilized. Whereas the former lacks the HUB finger, the latter possesses neither the HUB finger nor the SE14 repeat domain (Fig. 1*A*). Full-length hHDAC6 and these two mutants were expressed in 293 cells as FLAG-tagged proteins. Extracts were prepared and subjected to sizing chromatography as described above. As shown in Fig. 2*B* (*lower three panels*), like endogenous HDAC6 from HeLa S3 cells, FLAG-tagged hHDAC6 migrated on the Superose 6 column as an ~500-kDa species. Mutant 1–1043 was detected as a peak slightly smaller than hHDAC6, suggesting that the HUB domain does not grossly affect the migration of hHDAC6 on the gel filtration column. By contrast, mutant 1–888 peaked at fraction 30, corresponding to ~150 kDa, suggesting that the SE14 repeat domain is responsible for the anomalous migration of hHDAC6 in size-exclusion chromatography. These results indicate that the SE14 repeat domain may form an unusual structure and affect the overall structure of hHDAC6.

Requirement of the SE14 Repeat Domain for Deacetylase Activities of hHDAC6—We next investigated whether the SE14 repeat domain affects functions of hHDAC6. For this, FLAG-tagged hHDAC6 was expressed in Sf9 cells and affinity-purified to near-homogeneity. As shown in Fig. 2*D*, the purified hHDAC6 protein possessed similar activity as that expressed in and affinity-purified from 293T cells. To assess how the SE14 repeat domain might affect the HDAC activity of hHDAC6, we analyzed the deletion mutants 1–1043 and 1–888. As shown in Fig. 2*D*, both mutants were found to be as active as the full-length hHDAC6 proteins, indicating that the SE14 repeat domain is not required for the HDAC activity of hHDAC6.

Besides its deacetylase activity toward histones, HDAC6 also deacetylates α -tubulin (16, 18, 19, 21), so we asked whether the SE14 repeat domain regulates the tubulin deacetylase activity of hHDAC6. For this, BalbC3T3 cells were transfected with expression vectors for GFP-tagged hHDAC6 and mutant Δ SE14. In this mutant, residues 888–1024 were removed to delete the SE14 repeat domain. Cells expressing GFP-hHDAC6 or Δ SE14 were treated with 50 nM TSA and analyzed by fluorescence microscopy. As shown in Fig. 3*A*, like the wild-type HDAC6 protein, mutant Δ SE14 deacetylated α -tubulin in

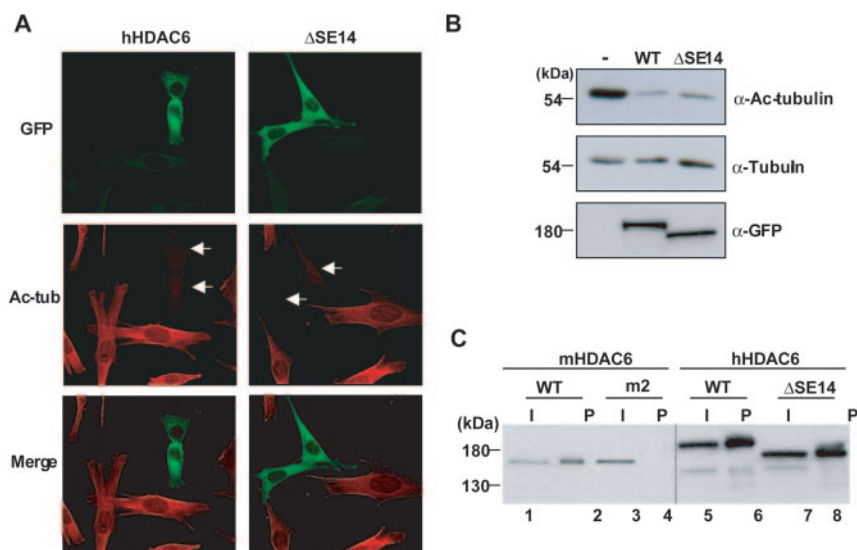


FIG. 3. The SE14 repeat domain of hHDAC6 is dispensable for tubulin deacetylation and ubiquitin binding. *A*, BalbC3T3 cells were transfected with a plasmid expressing GFP-hHDAC6 or GFP- Δ SE14. 24 h post-transfection, cells were treated with 50 nM TSA for 6 h and fixed for fluorescence microscopy to detect GFP fusion proteins (green) and acetyl α -tubulin (red). Merged images are depicted at the bottom. Arrows indicate the disappearance of acetyl α -tubulin. *B*, COS cells were transfected with expression vectors for GFP-hHDAC6 or GFP- Δ SE14. 24 h post-transfection, cells were lysed and kept at room temperature for 30 min prior to addition of SDS-PAGE sample buffer. Immunoblotting was performed successively with anti-acetyl α -tubulin (upper panel), anti- α -tubulin (middle panel), and anti-GFP (lower panel). *C*, expression vectors for hemagglutinin-tagged mHDAC6 and mutant m2, and for GFP-tagged hHDAC6 and Δ SE14, were expressed in COS cells. 24 h post-transfection, cell extracts were prepared and incubated with ubiquitin-agarose beads. Proteins retained on the beads were eluted (*P*) and analyzed together with 10% of input (*I*) by Western blotting with anti-hemagglutinin (lanes 1–4) or anti-GFP (lanes 5–8) antibody. WT, wild type.

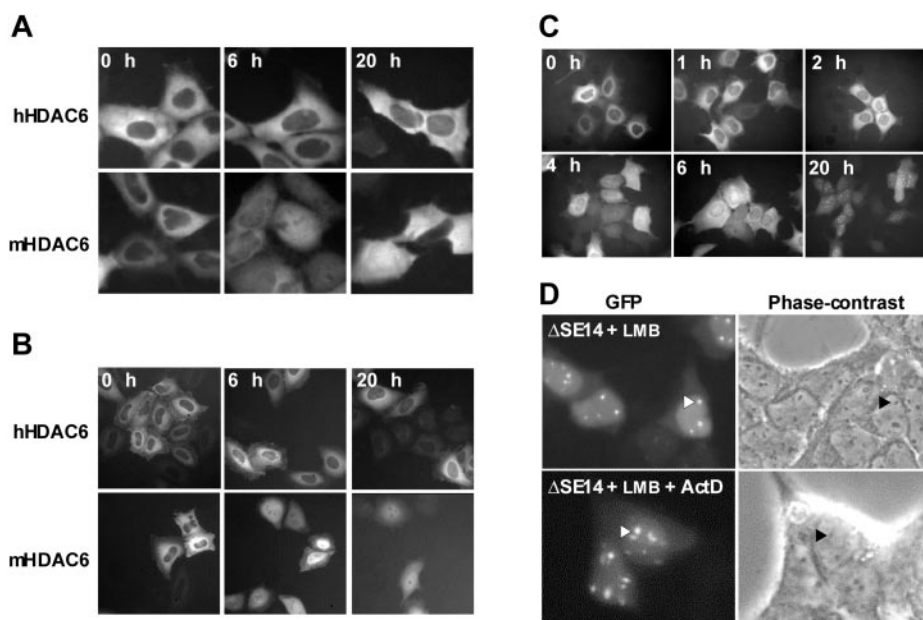


FIG. 4. The SE14 repeat domain of hHDAC6 mediates LMB resistance. *A* and *B*, 293 (*A*) and HeLa (*B*) cells expressing hHDAC6 and mHDAC6 as GFP fusion proteins were treated with 0.1 (*A*) or 0.02 μ M (*B*) LMB and analyzed by green fluorescence microscopy at the indicated time points. *C*, 293 cells expressing GFP- Δ SE14 were treated with 0.02 μ M LMB and analyzed by green fluorescence microscopy at the indicated time points. *D*, 293 cells expressing GFP- Δ SE14 were treated either with 0.02 μ M LMB for 17 h (top) or 0.02 μ M LMB for 17 h followed by 1.0 μ g/ml ActD for 2 h (bottom). The subcellular localization of GFP- Δ SE14 was assessed by live green fluorescence microscopy. Representative intense GFP signals (left) and the corresponding nucleoli (right) are indicated with light and dark arrowheads, respectively.

in vivo. Consistent with this, the wild-type and mutant HDAC6 proteins both efficiently deacetylated α -tubulin *in vitro* (Fig. 3*B*), indicating that the SE14 repeat domain is dispensable for the tubulin deacetylase activity of hHDAC6.

Role of the SE14 Repeat Domain in Ubiquitin Binding—The HUB finger of HDAC6 binds to ubiquitin (12, 13). Because of its close proximity to this finger (Fig. 1*A*), the SE14 repeat domain may affect the ubiquitin binding activity of hHDAC6. To address this, mouse and human HDAC6 proteins were expressed in COS cells, and extracts were tested for the ability to bind

ubiquitin-agarose. As a control, we tested mHDAC6 and its point mutant, m2, in which His-1094 and His-1098, residues critical for ubiquitin binding, are replaced with alanine (12). As reported (12), wild-type mHDAC6, but not m2, was retained on ubiquitin-agarose (Fig. 3*C*, lanes 1–4). Wild-type hHDAC6 and mutant Δ SE14 were retained on the agarose to similar levels (Fig. 3*C*, lanes 5–8), indicating that the SE14 repeat domain does not affect the ubiquitin binding ability of hHDAC6. Moreover, the SE14 repeat domain itself did not bind to ubiquitin (data not shown).

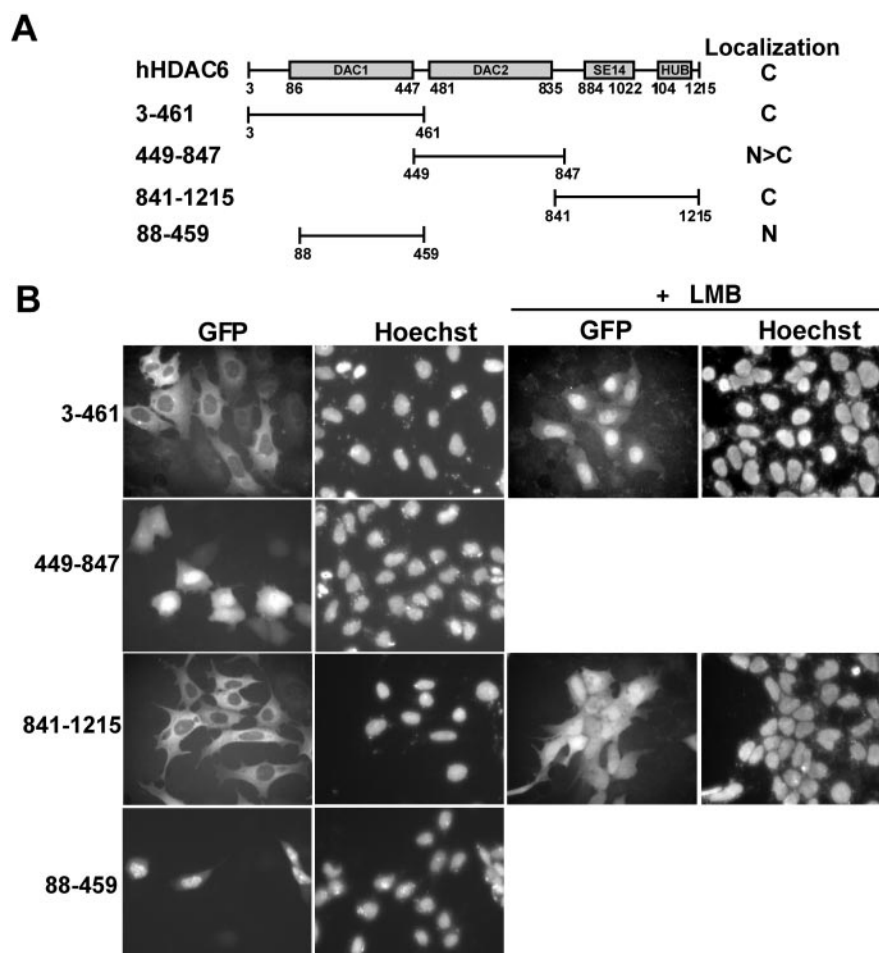


FIG. 5. hHDAC6 possesses motifs with nuclear import and export activities. *A*, schematic representation of hHDAC6 deletion mutants with their subcellular localization summarized at right: *C*, predominantly cytoplasmic; *N>C*, partially enriched in the nucleus; and *N*, predominantly nuclear. *B*, 293 cells expressing the indicated deletion mutants as GFP fusion proteins were fixed, stained with Hoechst 33258, and examined under a fluorescence microscope. For assessment of CRM1-dependent nuclear export, transfected cells were incubated with 0.02 μ M LMB for 17 h prior to fixation.

LMB-resistant Cytoplasmic Localization of hHDAC6—mHDAC6 is mainly cytoplasmic (23), so we examined the subcellular localization of hHDAC6. For this, nuclear and cytoplasmic extracts were prepared from 293, 293T, and HeLa cells. Immunoblotting analysis of these extracts with a polyclonal antibody raised against the C-terminal third of hHDAC6 revealed that endogenous hHDAC6 was predominantly cytoplasmic (data not shown). Moreover, GFP-hHDAC6 was found to be mainly cytoplasmic in 293 and HeLa cells (Fig. 4, *A* and *B*). Therefore, like mHDAC6, hHDAC6 is a cytoplasmic protein.

mHDAC6 is actively exported from the nucleus in a CRM1-dependent manner (23), so we asked whether hHDAC6 is similarly regulated. To address this question, 293 and HeLa cells expressing GFP-hHDAC6 were treated with LMB (30). Unexpectedly, the cytoplasmic localization of GFP-hHDAC6 was minimally affected by this treatment (Fig. 4, *A* and *B*). As reported (23), LMB treatment stimulated the nuclear accumulation of GFP-mHDAC6 (Fig. 4, *A* and *B*). These results indicate that the cytoplasmic localization of hHDAC6 is controlled differently from that of mHDAC6.

Role of the SE14 Repeat Domain in LMB-resistant Cytoplasmic Localization of hHDAC6—The SE14 repeat domain is the major difference between murine and human HDAC6 proteins (Fig. 1*A*). To determine whether this domain regulates the cytoplasmic retention of hHDAC6, mutant Δ SE14 was expressed as a GFP fusion protein in 293 cells, and its subcellular localization was examined by fluorescence microscopy. Without LMB treatment, GFP- Δ SE14 was mainly cytoplasmic in 293 cells (Fig. 4*C*). 2 h after LMB treatment, GFP- Δ SE14 started to enter the nucleus; at 4–6 h, it became almost pan-cellular; and at 20 h, it was enriched in visible nuclear dots. These dots

appeared to be nucleoli (Fig. 4*D*, top). To understand how Δ SE14 is associated with subnucleolar compartments, 293 cells expressing GFP- Δ SE14 were treated with LMB along with 1 μ g/ml actinomycin D (ActD). At this concentration, ActD leads to segregation and subsequent dispersal of nucleolar compartments (31). As shown in Fig. 4*D* (bottom), GFP- Δ SE14 remained associated with punctate structures corresponding to compacted nucleoli that are known to contain condensed nucleolar chromatin. These results indicate that the SE14 repeat domain of hHDAC6 is required for LMB-resistant cytoplasmic localization.

Cytoplasmic Retention and Nuclear Export Signals of hHDAC6—Because the cytoplasmic localization of mutant Δ SE14 was sensitive to LMB treatment (Fig. 4*C*), hHDAC6 may possess a CRM1-dependent NES(s). Because mutant Δ SE14 is able to relocate to the nucleus (Fig. 4*C*), hHDAC6 may possess an NLS(s). Consistent with these contentions, mHDAC6 is subject to active nucleocytoplasmic trafficking and possesses a functional NES (23). To determine whether the LMB-resistant cytoplasmic localization of hHDAC6 is due to lack of nucleocytoplasmic trafficking signals and to analyze how the SE14 repeat domain contributes to the cytoplasmic localization of hHDAC6, we took a systematic approach to map related sequence determinants. Compared with full-length hHDAC6, mutant Δ SE14 is more similar to mHDAC6 at the structural level (Fig. 1*A*). Like mHDAC6 (23), Δ SE14 is subject to active nuclear export (Fig. 4*C*), suggesting that this mutant possesses nuclear import and export signals. To map these signals, we analyzed the deletion mutants 3–461, 449–847, and 841–1215 (Fig. 5*A*). As shown in Fig. 5*B*, 3–461 and 841–1215, but not 449–847, were mainly cytoplasmic. LMB treat-

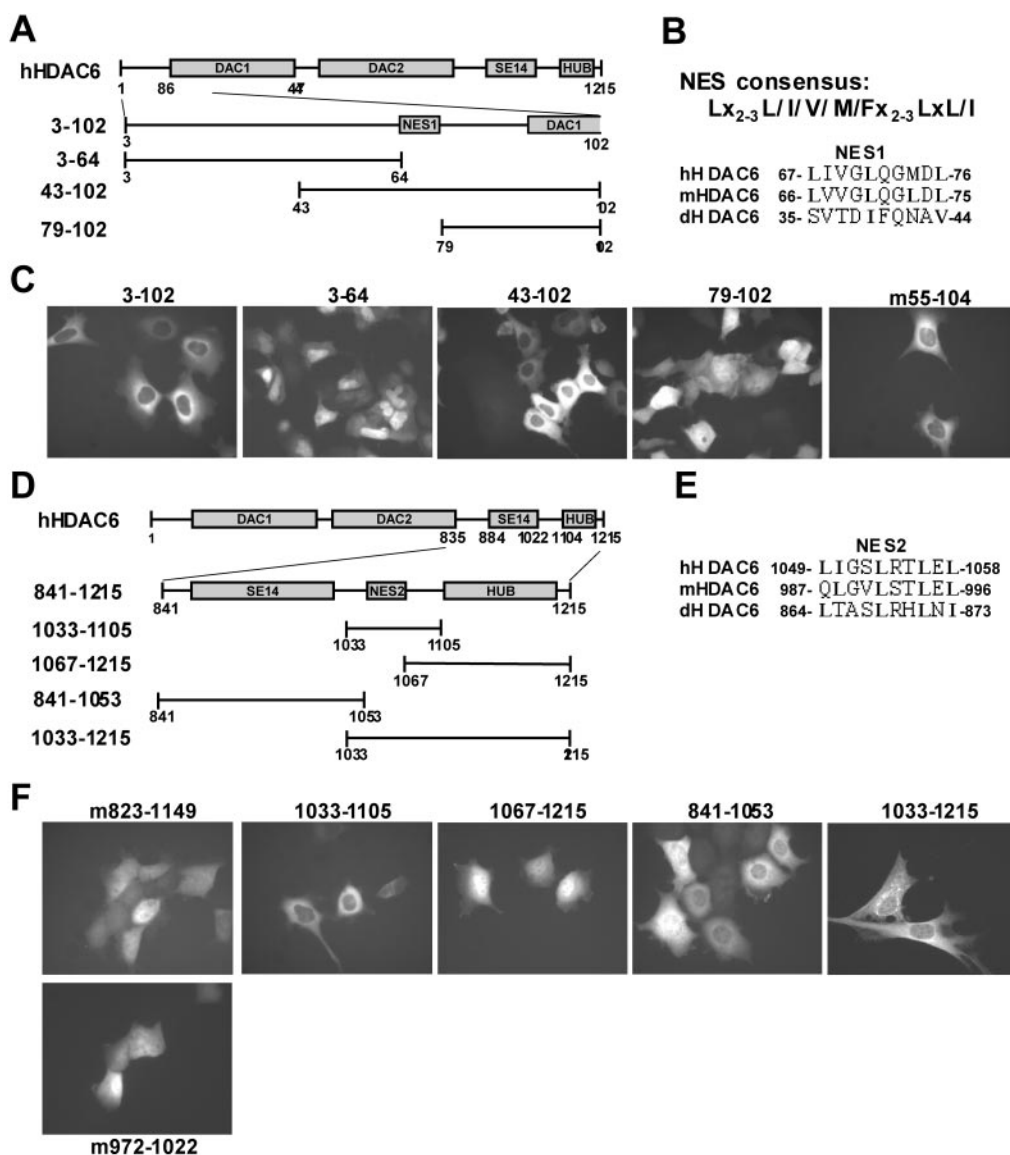


FIG. 6. Mapping of cytoplasmic retention and nuclear export sequences. *A*, schematic illustration of hHDAC6 deletion mutants used to map NES1. *B*, sequence alignment of hHDAC6 NES1 with the corresponding regions of mHDAC6 and dHDAC6. Residues matching the NES consensus sequence (depicted at top: *x* denotes any residue) are shown in **boldface**. *C*, 293 cells expressing the indicated deletion mutants as GFP fusion proteins were analyzed by live green fluorescence microscopy. *D*, schematic illustration of hHDAC6 deletion mutants used to map NES2. *E*, sequence alignment of NES2 with the corresponding regions of mHDAC6 and dHDAC6. Residues matching the NES consensus sequence are indicated in **boldface**. *F*, 293 cells expressing the indicated deletion mutants as GFP fusion proteins were analyzed by live green fluorescence microscopy.

ment led to nuclear accumulation of 3–461 (Fig. 5*B*), suggesting that it contains nuclear import and export signals. The same treatment led to pancellular distribution of 841–1215 (Fig. 5*B*), so it possesses an NES.

Unlike 3–461, mutant 88–459 was mainly nuclear (Fig. 5), indicating that an NES is located within the N-terminal 88 residues. Moreover, different from 3–102, 3–64 was nuclear (Fig. 6, *A* and *C*), so the NES is located between residues 64 and 88. The consensus sequence of known leucine-rich NESs is $LX_{2-3}L/I/V/M/FX_{2-3}LXL/I$, where *X* denotes any residue (32, 33). Inspection of the hHDAC6 sequence revealed that residues 67–76 constitute a putative NES (Fig. 6*B*, NES1). Upon treatment with LMB for 15 min, mutant 3–102 accumulated in the nucleus (data not shown), suggesting that its nuclear export occurs in a CRM1-dependent manner. To map the NES, mutants 43–102 and 79–102 (Fig. 6, *A* and *C*) were expressed as GFP fusion proteins and subjected to fluorescence microscopy. As shown in Fig. 6*C*, 43–102 was mainly cytoplasmic, unlike

79–102, indicating that residues 65–78 are important for the cytoplasmic localization. Substitution of Leu-76 with alanine inhibited the cytoplasmic localization of a deletion mutant containing the N-terminal 145 residues of hHDAC6 (data not shown). Therefore, NES1 constitutes a functional export signal. Consistent with this, a similar sequence is present in mHDAC6 (Fig. 6*B*) and functions as an NES (Fig. 6*C*, *m55-104*) (23).

Mutant 841–1215 was predominantly cytoplasmic (Fig. 5*B*). By contrast, the corresponding fragment of mHDAC6 was pancellular (Fig. 6*F*, *mHDAC6* mutant *m823-1149*). These findings further support the conclusion that residues 841–1215 of hHDAC6 possess an NES(s). Sequence inspection revealed a potential leucine-rich NES within this region (Fig. 6*E*, NES2), which matches the aforementioned consensus NES sequence (32, 33). To test whether NES2 is functional, four deletion mutants (Fig. 6*D*, *1033-1105*, *1067-1215*, *841-1053*, and *1033-1215*) were expressed as GFP fusion proteins and analyzed by green fluorescence microscopy. As shown in Fig. 6*F*, like 841–

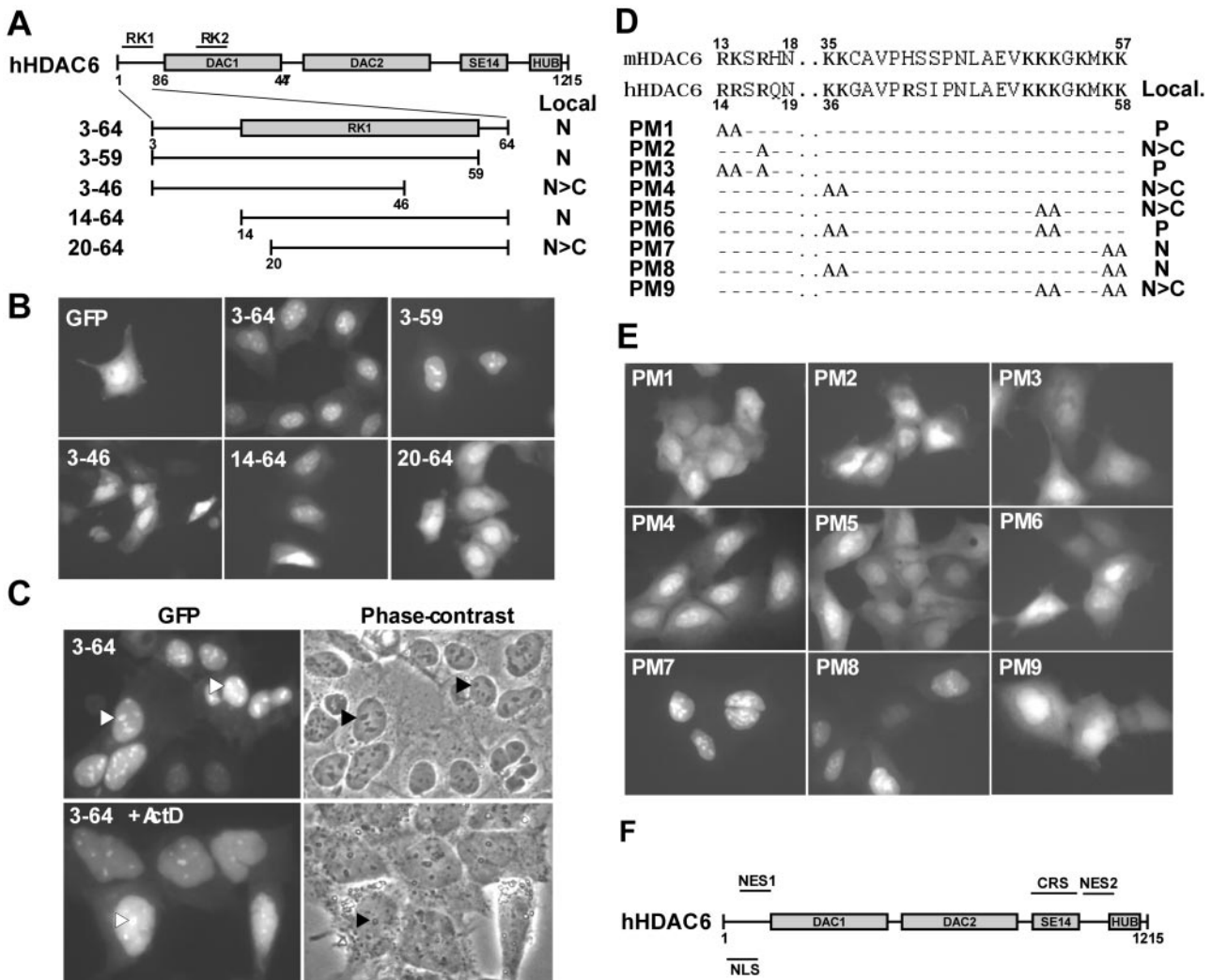


FIG. 7. Mapping of an NLS. *A*, schematic representation of hHDAC6 deletion mutants. Subcellular localization is summarized at *right*: *N*, predominantly nuclear and *N>C*, partially enriched in the nucleus. Also indicated are two arginine/lysine-rich clusters: *RK1*, residues 14–58, and *RK2*, residues 241–246 (KHRIRR). *B*, the indicated deletion mutants were expressed in 293 cells as GFP fusion proteins, and their subcellular localization was determined by live green fluorescence microscopy. *C*, comparison of the green fluorescence image (*left*) with the corresponding phase-contrast micrograph (*right*) of 293 cells expressing mutant 3–64 as a GFP fusion protein. Representative intense GFP signals and the corresponding nucleoli are denoted with *light* and *dark* arrowheads, respectively. ActD treatment was performed as in Fig. 4*D*. *D*, schematic representation of point mutants (*PM*) derived from mutant 3–64. Subcellular localization of the point mutants is summarized at *right*: *P*, pancellular; *N*, predominantly nuclear; and *N>C*, partially enriched in the nucleus. *E*, the indicated point mutants were expressed in 293 cells as GFP fusion proteins, and their subcellular localization was assessed by live green fluorescence microscopy. *F*, schematic representation of sequence elements controlling the subcellular localization of hHDAC6. Besides the indicated NLS, DAC1 also exhibits potent nuclear localization activity (Fig. 4), but this does not appear to be dependent on the arginine/lysine-rich motif RK2.

1215, 1033–1105 and 1033–1215 were cytoplasmic, suggesting that NES2 is functional. Consistent with this, 1067–1215 was pan-cellular (Fig. 6*F*). After a brief exposure to LMB, 1033–1105 became pan-cellular (data not shown), indicating that the nuclear export by NES2 occurs in a CRM1-dependent manner. Therefore, hHDAC6 possesses two leucine-rich nuclear export sequences.

Although GFP itself was slightly enriched in the nucleus (data not shown), mutant 841–1053 fused to GFP was slightly enriched in the cytoplasm (Fig. 6*F*), indicating that the SE14 repeat domain exhibits cytoplasmic retention activity. These results also suggest that NES2 and the SE14 repeat domain both contribute to the cytoplasmic localization activity of the C-terminal part of hHDAC6. Unlike mutant 1033–1105, the corresponding region of mHDAC6 did not exhibit such an activity (Fig. 6*F*, mHDAC6 mutant *m972–1022*). Therefore, compared with mHDAC6, hHDAC6 contains additional sequence determinants (*i.e.* the SE14 repeat domain and NES2) for cytoplasmic retention.

Nuclear Localization Signal of HDAC6—Upon LMB treatment, mutant 3–461 became nuclear (Fig. 5), so it possesses a potential NLS(s). Although 88–459 was enriched in the nucleus (Fig. 5), 3–102 was cytoplasmic (Fig. 6). Examination of the amino acid sequence of mutant 3–461 revealed two clusters rich in arginine and lysine residues (Fig. 7*A*, *RK1* and *RK2*) (34). Because 88–459 was nuclear, we first characterized *RK2*. Alanine substitution of residues 245–246 did not affect the nuclear localization of 88–459 (data not shown), indicating that *RK2* is nonfunctional. This finding prompted us to analyze *RK1*. As shown in Fig. 7, *B* and *C*, mutant 3–64 was enriched in the nucleus, especially in the dots corresponding to nucleoli, suggesting that *RK1* functions as an NLS and contributes to the nucleolar localization of Δ SE14 (Fig. 4). Consistent with this, as observed with Δ SE14, ActD treatment did not alter the association of 3–64 with nucleoli (Fig. 7*C*).

To characterize further the nuclear localization activity of *RK1*, four deletion mutants (Fig. 7*A*, 3–59, 3–46, 14–64, and 20–64) were tested. As shown in Fig. 7*B*, mutants 3–59 and

14–64 were nuclear, whereas 3–46 and 20–64 exhibited more intense signals in the cytoplasm, suggesting that residues 14–19 and 47–64 are important elements of RK1. Mutant 3–59 was more nuclear than 3–64 (Fig. 7B), so residues 60–64 may negatively regulate the nuclear import function. To characterize RK1 further, selected basic residues conserved in mHDAC6 were substituted with alanine (Fig. 7D). The resulting mutants were expressed in 293 cells and analyzed by live green fluorescence microscopy. As shown in Fig. 7, D and E, substitution of RR14–15 dramatically decreased the nuclear localization, whereas replacement of R17 or KK36–37 with alanine had smaller effects (compare the point mutants PM1–4 with 3–64). Substitution of 52–53 also decreased the nuclear localization (compare the point mutant PM5 with 3–64). Consistent with this, mutant PM6 was almost pancellular, whereas PM4 was enriched in the nucleus. Most surprisingly, replacement of KK57–58 increased the nuclear localization (compare mutants PM7 and PM8 with 3–64 and PM4, respectively). This is consistent with the observation that 3–59 was more nuclear than 3–64 (Fig. 7B). The point mutant PM9 was less nuclear than PM7 (Fig. 7, D and E), confirming the importance of KK52–53. Together, these results suggest that RK1 of hHDAC6 constitutes a functional NLS. Consistent with this, deletion of RK1 in full-length mHDAC6 delayed its nuclear entry upon LMB treatment (data not shown). Therefore, RK1 of HDAC6 functions as an NLS.

DISCUSSION

The SE14 Repeat Domain Functions as a CRS—The results presented here indicate that hHDAC6 possesses a unique SE14 repeat domain that is missing in HDAC6 proteins from *C. elegans*, *Drosophila*, mouse, and rat (Fig. 1). Like mHDAC6 (23), hHDAC6 is mainly cytoplasmic (Fig. 4) (16, 18–21). Unlike that of mHDAC6 (23), the cytoplasmic localization of hHDAC6 is LMB-resistant (Fig. 4), indicative of differential regulation for the cytoplasmic localization of murine and human HDAC6 proteins. The SE14 repeat domain is required for the LMB resistance (Fig. 4) and is also responsible for the anomalous migration of hHDAC6 in size-exclusion chromatography (Fig. 2). Moreover, fragment 841–1053 was able to target GFP to the cytoplasm (Fig. 6). This fragment also displays weak microtubule targeting activity (data not shown). Therefore, the SE14 repeat domain is a CRS that is important for modulating the cytoplasmic localization of hHDAC6.

HDAC6 Possesses Sequences with Nuclear Import and Export Activities—Besides the SE14 repeat domain, hHDAC6 possesses potential nuclear import and export sequences (Fig. 7F). It has two potent leucine-rich export signals, residues 67–76 and 1049–1058 (Figs. 6 and 7F, NES1 and NES2, respectively). Upon treatment with the CRM1-specific inhibitor LMB, mutants 3–102 and 1033–1105 rapidly relocated to the nucleus (~15 min; data not shown), so both NES1 and NES2 can function as potent CRM1-dependent export signals. NES1 is highly conserved in mHDAC6 (Fig. 6B), and the corresponding region has been identified as an NES (Fig. 6C, m55–104) (23). By contrast, NES2 is less conserved in mHDAC6 (Fig. 6E), and the corresponding region has been found to be nonfunctional in nuclear export (Fig. 6F, m972–1022) (23). Most interestingly, NES2, but not NES1, is conserved in dHDAC6 (Fig. 6, B and E) (29), so the region corresponding to dHDAC6 may function as an NES. Related to this, dHDAC6 is mainly cytoplasmic (29). Therefore, different HDAC6 proteins contain distinct NESs.

When fused to GFP, RK1 of hHDAC6 functioned as an NLS (Fig. 7). Compared with known nuclear import signals, this NLS is atypical. RR14–15 and KK52–53 are key elements, whereas R17 and KK36–37 play less important roles (Fig. 7, D and E). Such an organization is distinct from classical mono-

partite or bipartite NLSs (34–36). Residues 57–64 negatively regulate the function of RK1 (Fig. 7). RK1 displays nucleolus targeting activity. Like RK1, several known nucleolar localization signals are R/K-rich (37, 38). RK1 of hHDAC6 is well conserved in mHDAC6 (Fig. 7D), and mHDAC6 is actively shuttled between the nuclear and cytoplasmic compartments (Fig. 4) (23), indicating that RK1 may be involved in the nuclear import of mHDAC6. By contrast, dHDAC6 does not have a similar sequence (29), suggesting that RK1-directed activity is unique to HDAC6 proteins from higher organisms.

The identification of sequences with nuclear import and export activities (Figs. 6 and 7) suggests two possibilities. The first one is that the subcellular localization of hHDAC6 is regulated. Consistent with this, LMB treatment led to nuclear accumulation of mHDAC6 (Fig. 4, A and B) (23). In addition, HDAC6 has been shown to interact with nuclear proteins such as HDAC11 (39), the transcriptional corepressors ETO2 and L-CoR (40, 41), the runt-domain transcription factor Runx2 (42), and sumoylated p300 (43). The second possibility is that the import and export sequences are recognized by importin and exportin for cellular processes other than nucleocytoplasmic trafficking (44, 45). CRM1 is involved in regulating DNA replication (45) and importin α/β transports protein targets with basic NLSs to the proximity of mitotic chromosomes (44, 46–48). Of relevance, HDAC6 associates with special microtubule structures such as the microtubule organization centers and the midbody (19, 20). The results presented here thus pave the way for further investigation to distinguish between these intriguing possibilities.

REFERENCES

1. Yang, X. J. (2004) *BioEssays* **26**, 1076–1087
2. Cress, W. D., and Seto, E. (2000) *J. Cell. Physiol.* **184**, 1–16
3. Khochbin, S., Verdel, A., Lemerrier, C., and Seigneurin-Berny, D. (2001) *Curr. Opin. Genet. Dev.* **11**, 162–166
4. Grozinger, C. M., and Schreiber, S. L. (2002) *Chem. Biol.* **9**, 3–16
5. Verdin, E., Dequiedt, F., and Kasler, H. G. (2003) *Trends Genet.* **19**, 286–293
6. Rundlett, S. E., Carmen, A. A., Kobayashi, R., Bavykin, S., Turner, B. M., and Grunstein, M. (1996) *Proc. Natl. Acad. Sci. U. S. A.* **93**, 14503–14508
7. McKinsey, T. A., Zhang, C. L., and Olson, E. N. (2002) *Trends Biochem. Sci.* **27**, 40–47
8. Verdel, A., and Khochbin, S. (1999) *J. Biol. Chem.* **274**, 2440–2445
9. Grozinger, C. M., Hassig, C. A., and Schreiber, S. L. (1999) *Proc. Natl. Acad. Sci. U. S. A.* **96**, 4868–4873
10. Amerik, A. Y., Li, S. J., and Hochstrasser, M. (2000) *Biol. Chem.* **381**, 981–992
11. Bertos, N. R., Wang, A. H., and Yang, X. J. (2001) *Biochem. Cell Biol.* **79**, 243–252
12. Seigneurin-Berny, D., Verdel, A., Curtet, S., Lemerrier, C., Garin, J., Rousseaux, S., and Khochbin, S. (2001) *Mol. Cell. Biol.* **21**, 8035–8044
13. Hook, S. S., Orfan, A., Cowley, S. M., and Eisenman, R. N. (2002) *Proc. Natl. Acad. Sci. U. S. A.* **99**, 13425–13430
14. Kawaguchi, Y., Kovacs, J. J., McLaurin, A., Vance, J. M., Ito, A., and Yao, T. P. (2003) *Cell* **115**, 727–738
15. Kovacs, J. J., Hubbert, C., and Yao, T. P. (2004) *Novartis Found Symp.* **259**, 170–177
16. Hubbert, C., Guardiola, A., Shao, R., Kawaguchi, Y., Ito, A., Nixon, A., Yoshida, M., Wang, X. F., and Yao, T. P. (2002) *Nature* **417**, 455–458
17. Palazzo, A., Ackerman, B., and Gundersen, G. G. (2002) *Nature* **421**, 230
18. Matsuyama, A., Shimazu, T., Sumida, Y., Saito, A., Yoshimatsu, Y., Seigneurin-Berny, D., Osada, H., Komatsu, Y., Nishino, N., Khochbin, S., Horinouchi, S., and Yoshida, M. (2002) *EMBO J.* **21**, 6820–6831
19. Zhang, Y., Li, N., Caron, C., Matthias, G., Hess, D., Khochbin, S., and Matthias, P. (2003) *EMBO J.* **22**, 1168–1179
20. Haggarty, S. J., Koeller, K. M., Wong, J. C., Grozinger, C. M., and Schreiber, S. L. (2003) *Proc. Natl. Acad. Sci. U. S. A.* **100**, 4389–4394
21. North, B. J., Marshall, B. L., Borra, M. T., Denu, J. M., and Verdin, E. (2003) *Mol. Cell* **11**, 437–444
22. Serrador, J. M., Cabrero, J. R., Sancho, D., Mittelbrunn, M., Urzainqui, A., and Sanchez-Madrid, F. (2004) *Immunity* **20**, 417–428
23. Verdel, A., Curtet, S., Brocard, M. P., Rousseaux, S., Lemerrier, C., Yoshida, M., and Khochbin, S. (2000) *Curr. Biol.* **10**, 747–749
24. Dignam, J. D., Lebovitz, R. M., and Roeder, R. G. (1983) *Nucleic Acids Res.* **11**, 1475–1489
25. Wang, A. H., Bertos, N. R., Vezmar, M., Pelletier, N., Crosato, M., Heng, H. H., Th'ng, J., Han, J., and Yang, X. J. (1999) *Mol. Cell. Biol.* **19**, 7816–7827
26. Wang, A. H., Kruhlik, M. J., Wu, J., Bertos, N. R., Vezmar, M., Posner, B. I., Bazett-Jones, D. P., and Yang, X. J. (2000) *Mol. Cell. Biol.* **20**, 6904–6912
27. Champagne, N., Bertos, N. R., Pelletier, N., Wang, A. H., Vezmar, M., Yang, Y., Heng, H. H., and Yang, X. J. (1999) *J. Biol. Chem.* **274**, 28528–28536
28. Wang, A. H., and Yang, X. J. (2001) *Mol. Cell. Biol.* **21**, 5992–6005
29. Barlow, A. L., van Drunen, C. M., Johnson, C. A., Tweedie, S., Bird, A., and

- Turner, B. M. (2001) *Exp. Cell Res.* **265**, 90–103
30. Kudo, N., Matsumori, N., Taoka, H., Fujiwara, D., Schreiner, E. P., Wolff, B., Yoshida, M., and Horinouchi, S. (1999) *Proc. Natl. Acad. Sci. U. S. A.* **96**, 9112–9117
31. LaMorte, V. J., Dyck, J. A., Ochs, R. L., and Evans, R. M. (1998) *Proc. Natl. Acad. Sci. U. S. A.* **95**, 4991–4996
32. Bogerd, H. P., Fridell, R. A., Benson, R. E., Hua, J., and Cullen, B. R. (1996) *Mol. Cell. Biol.* **16**, 4207–4214
33. Murphy, R., and Wenthe, S. R. (1996) *Nature* **383**, 357–360
34. Dingwall, C., and Laskey, R. A. (1991) *Trends Biochem. Sci.* **16**, 478–481
35. Nakielny, S., and Dreyfuss, G. (1999) *Cell* **99**, 677–690
36. Kalderon, D., Roberts, B. L., Richardson, W. D., and Smith, A. E. (1984) *Cell* **39**, 499–509
37. Perkins, A., Cochrane, A. W., Ruben, S. M., and Rosen, C. A. (1989) *J. Acquired Immune Defic. Syndr.* **2**, 256–263
38. Scott, M., Boisvert, F. M., Vieyra, D., Johnston, R. N., Bazett-Jones, D. P., and Riabowol, K. (2001) *Nucleic Acids Res.* **29**, 2052–2058
39. Gao, L., Cueto, M. A., Asselbergs, F., and Atadja, P. (2002) *J. Biol. Chem.* **277**, 25748–25755
40. Amann, J. M., Nip, J., Strom, D. K., Lutterbach, B., Harada, H., Lenny, N., Downing, J. R., Meyers, S., and Hiebert, S. W. (2001) *Mol. Cell. Biol.* **21**, 6470–6483
41. Fernandes, I., Bastien, Y., Wai, T., Nygard, K., Lin, R., Cormier, O., Lee, H. S., Eng, F., Betos, N. R., Pelletier, N., Mader, S., Han, V. K. M., Yang, X.-J., and White, J. H. (2003) *Mol. Cell* **11**, 139–150
42. Westendorf, J. J., Zaidi, S. K., Cascino, J. E., Kahler, R., van Wijnen, A. J., Lian, J. B., Yoshida, M., Stein, G. S., and Li, X. (2002) *Mol. Cell. Biol.* **22**, 7982–7992
43. Girdwood, D., Bumpass, D., Vaughan, O. A., Thain, A., Anderson, L. A., Snowden, A. W., Garcia-Wilson, E., Perkins, N. D., and Hay, R. T. (2003) *Mol. Cell* **11**, 1043–1054
44. Wiese, C., Wilde, A., Moore, M. S., Adam, S. A., Merdes, A., and Zheng, Y. (2001) *Science* **291**, 653–656
45. Yamaguchi, R., and Newport, J. (2003) *Cell* **113**, 115–125
46. Dasso, M. (2001) *Cell* **104**, 321–324
47. Nachury, M. V., Maresca, T. J., Salmon, W. C., Waterman-Storer, C. M., Heald, R., and Weis, K. (2001) *Cell* **104**, 95–106
48. Schatz, C. A., Santarella, R., Hoenger, A., Karsenti, E., Mattaj, I. W., Gruss, O. J., and Carazo-Salas, R. E. (2003) *EMBO J.* **22**, 2060–2070